Journal of Engg. Research **Vol. 4 No. (4) December 2016** pp. 194-213

التصادم غير المرن ومعامل الرد

أندرياس كرستفورو وأهمت يجيت
قسم الهندسة الميكانيكية، كلية الهندسة والبترول، جامعة الكويت، الكويت

الخلاصة

يقوم هذا البحث على طرح نموذج يؤدي الى فهم تأثير تصادم جسم كروي مشوه مع سطح مستوي. ويتضمن النموذج عنصر تلامس غير خطي لحساب الطاقة المفقودة نتيجة التشوه البلاستيكي أو التسطيح للجسم الكروي وعنصر لزج لحساب الطاقة المفقودة نتيجة انتشار الموجات وتخميدها وكذلك عنصر صلابة خطي لحساب آثار الارتداد خلال وبعد التصادم. وسوف تستخدم نسخة خطية معدلة للنموذج وذلك لتبسيط تطبيع المعادلات مع توفير رؤية مفيدة لمسألة التصادم. وتوضح النتائج ان نتيجة التصادم يمكن نسبتها الى عاملين ليس لهما بعد، الصلابة النسبية، λ ، الذي يحسب آثار الارتداد، التشوه البلاستيكي أو التسطيح للجسم الكروي، وكذلك معامل التخميد، ξ، الذي يحسب آثار اللزوجة و/ أو انتشار الموجات وتخميدها. توقعات النموذج تتوافق بشكل جيد مع النتائج المخبرية للكرات الرياضية التي تعتبر أمثلة ممتازة للأجسام الكروية المشوهة. قوة التصادم السوي ومعامل الرد (COR) تعتمد على هذين العاملين. عند سرعات ومعاملات تخميد منخفضة، تعتمد قوة التصادم السوي ومعامل الرد (COR) بشكل رئيسي على التخميد، بينما عند سرعات منخفضة ومعاملات تخميد مرتفعة، تعتمد على التخميد والمرونة. فمثلا بنسبة تخميد محددة فإن قوة التصادم السوي القصوى ومعامل الرد (COR) تقل مع زيادة المرونة. اعتمادًا على خصائص تشوه الكرة في السرعات العالية، يقل معامل الرد (COR) بشكل أكبر نتيجة آثار تسوية السطح.

Inelastic impact and the coefficient of restitution

Andreas P. Christoforou* and Ahmet S. Yigit

Department of Mechanical Engineering, Kuwait University

**Corresponding author: andreas.christoforou@ku.edu.kw*

ABSTRACT

A model for the impact between a structurally deformable sphere and a rigid flat surface is presented. It includes a nonlinear contact element that accounts for energy loss due to local plastic deformation or flattening of the sphere, a viscous element that accounts for energy loss due to wave propagation and/or damping, and a linear stiffness element that accounts for recoil effects during and after impact. A linearized version of the model facilitates normalization of the equations with helpful insights into the impact problem. The results show that the impact event can be characterized by two non-dimensional parameters, namely the relative stiffness λ, which accounts for recoil effects, plastic deformation and/or flattening of the sphere, and the damping factor, ζ, which accounts for viscous and/or wave propagation effects. Model predictions compare well with experimental data for sports balls that are excellent examples of deformable spheres. The normalized impact force and the coefficient of restitution (COR) are dependent on both parameters. At low speeds and damping factors the normalized impact force and COR mainly depend on damping, whereas, at low speeds and large damping factors they depend on damping and flexibility. For a given damping factor, the normalized maximum impact force and COR decrease with higher flexibility. Depending on the deformation characteristics of the ball, at higher speeds the COR decreases further due to surface flattening effects.

Keywords: Coefficient of restitution; deformable compact bodies; impact dynamics.

INTRODUCTION

One of the most important areas of everyday living is sports, where in most cases different type of balls are used. In many cases, the balls are deformable spheres, and depending on the type of the sport, it involves impact with, a human being, appropriate sport equipment that launch the ball, or the ground of a playing field. In designing these balls and the corresponding equipment, it is important to understand the impact dynamics of the ball with various targets or sources of momentum transfer. Accurate knowledge of the impact response of sports balls leads to improvements in performance as well as safety. As a result extensive research on the subject has been performed

(Cross, 1999; Goodwill et al., 2005; Strong & Ashcroft, 2007; Ranga & Strangwood, 2010; Ismail & Strong, 2012; Hanly et al., 2012; Alsakarneh et al., 2012; Nevins & Smith, 2013; Smith & Burbank, 2013), ranging from experimental studies, simple and complicated analytical models to more sophisticated finite element (FE) techniques.

The impact dynamics of a sport ball is a complicated event that depends on the type of the ball. Cross (1999) presented an experimental study of the dynamics of a bouncing ball for several sports balls. He presented measurements of nonlinear force-displacement hysteresis curves, force-time and displacement-time response curves, and the COR, for a tennis ball, a baseball, a golf ball, a superball, a steel bearing, a plasticine ball, and a silly putty ball. He observed that most balls rebounded in a slightly compressed state with the energy loss occurring during the bounce. Goodwill et al. (2005) presented a study for the oblique and normal impact of a pressurized tennis ball on a rigid surface. They used a FE model and compared the simulations of the impact event with experiments. The results were in excellent agreement, demonstrating the complicated response of a pressurized ball, and the importance of accurately modeling material and structural parameters. Stronge & Achcroft (2007) presented a planar theory for impact of inflated balls with a rough rigid surface. The theory was developed on the assumption of a deformation field that has a flattened contact patch, and a reaction force, that is predominately due to internal gas pressure. With kinematic assumption, they were able to relate the geometry of the deformed ball with the indentation and contact force. Ranga & Strangwood (2010) presented a FE modeling and analysis for the dynamic behavior of a solid sports ball by using experimentally determined viscoelastic material properties. They concluded that viscoelastic material relaxation data are not suitable for the short times associated with the dynamic behavior of solid sports balls. Ismail & Stronge (2012) developed a viscoplastic compliance model that incorporates both elastic-plastic and viscoelastic material effects to analyze direct impact of sports balls. The analysis is based on a modified Maxwell model that utilizes experimental measurements of the contact force and COR to obtain the parameters of the viscoplastic compliance. Hanly et al. (2012) used linear and non-linear contact models to study the impact response of a sliotar core. They concluded that the Hunt-Crossley model (Hunt & Crossley, 1975) compared well with experimental data. Alsakarneh et al. (2012) used a modified Maxwell viscoelastic model to study the impact behavior and predict the COR of a sliotar. The correlations between the analytical predictions, developed FE model and experimental measurements of the COR were very good. Nevins & Smith (2013) demonstrated the importance of quantitative knowledge of how materials affect player safety by simulating ball-to-head impacts. They showed that the severity of injury strongly depends on ball material properties, which can differ significantly within similarly designed balls. Smith & Burbank (2013) showed that numerical predictions of solid sport ball impacts can be improved by using correct material models.

The main objective of this work is to present a nonlinear impact model for deformable spheres that captures most of the physics that affect the COR. It is inspired from the well-known standard solid or Zener model (Zener & Feshbach, 1939). It accounts for most energy dissipation effects seen in inelastic conditions, such as plasticity, viscous, and wave propagation effects. It also includes a linear stiffness element that accounts for recoil effects during and after contact. The proposed model predictions are compared to experimental measurements for several sports balls.

EQUATIONS OF MOTION FOR IMPACT

The impact between a deformable sphere having an initial velocity of v_0 with a flat rigid surface can be modeled as shown in Figure 1.

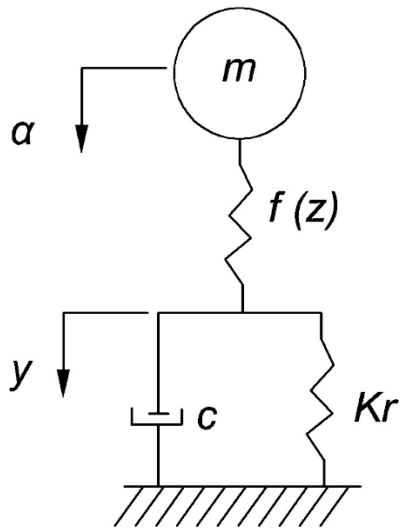

Fig. 1. Sketch of the proposed impact model

The motion of the sphere is described by,

$$m\ddot{\alpha} = -F \tag{1}$$

$$c\dot{y} + K_r y = F \tag{2}$$

where m is the mass of the sphere, α is the displacement of the sphere, c is the damping coefficient, which represents either viscous dissipation in the material, or the effect of energy dissipation due to wave propagation, y is the displacement of the viscous element, K_r is the recoil stiffness of the sphere, and F is the impact force to be obtained from a contact law given in general as,

$$F = \begin{cases} f(z) & if \quad F > 0 \\ 0 & if \quad F \le 0 \end{cases} \tag{3}$$

where z is the contact indentation defined as,

$$z = \alpha - y \tag{4}$$

The initial conditions are described as: $\alpha(0) = y(0) = 0$, and $\dot{\alpha}(0) = v_0$.

In cases where the energy dissipation is due to wave propagation, the damping coefficient c can be calculated as in Zener & Feshbach (1939); Goldsmith (1960); Doyle (1989) and Christoforou & Yigit (2009). In the case of an axial impact of a rigid sphere and a relatively long slender bar the energy is dissipated due to axial waves, and the damping coefficient is $c = A\sqrt{\rho E}$, where ρ and E are the material density and Young's modulus, respectively, and A is the cross sectional area of the bar. In the case of a transverse impact of a relatively large thin plate by a rigid sphere the energy is dissipated due to transverse waves and the damping coefficient is $c = 8\sqrt{\rho h D}$, where h is the thickness and D is the effective bending stiffness of the plate. According to Weir & Tallon (2005), most of the dissipated energy during impact in spherical objects is due to Rayleigh waves. Therefore, in a similar fashion to the cases mentioned above, the damping coefficient can be calculated as,

$$c = 0.94A\sqrt{\rho G} \tag{5}$$

where A is the surface area of the sphere, and G is the shear modulus.

The equations of motion can be solved numerically to obtain the impact response and determine the severity of impact by utilizing an appropriate contact law. The severity of impact can be assessed by the COR. There are three definitions, Newton (kinematic), Poisson (kinetic), and Energetic (Stronge, 2000). Depending on the problem, these definitions result in different values for the coefficient of restitution. However, in the case under study (normal impacts with no friction), all definitions give the same result. The Newton's definition for the coefficient of restitution is the simplest as it involves the ratio of the relative velocities of the impactor and the target after and before impact. It is simply given as,

$$e = -\frac{\dot{\alpha}(t_f)}{\dot{\alpha}(0)} \tag{6}$$

In the following sections three contact laws are presented, namely Hertz's contact law, an elastic-fully plastic contact law, and its linearized version. For spherical objects that are very compact and elastic in nature (i.e., ball bearings, billiards, bowling balls), the Hertz contact law can be used. In such cases impact is elastic and the COR is

unity. In metallic spheres, where permanent deformation may occur, the elastic-fully plastic contact law can be used. In such cases, depending on material and structural characteristics, the impact is inelastic and most of energy dissipation is due to localized plastic deformation. The COR may vary from unity to a lower value depending on the impact velocity. For the case at hand, i.e. impact of deformable spheres such as sports balls, the linearized contact law that takes into account wave propagation and large deformation effects (ball flattening) is used.

Hertz contact law

In cases where impacts are elastic in nature, (i.e. no plastic deformation or viscous effects) the classical Hertz contact theory (Goldsmith, 1960; Johnson, 1985: Stronge, 2000) may be used in Equation (3) to obtain the impact force. The relationship between the contact force and the relative contact deformation is given as,

$$F = K_h z^{3/2} \tag{7}$$

where K_h is the Hertzian contact stiffness given as,

$$K_h = \frac{4}{3}\sqrt{R}E^* \tag{8}$$

R is the radius of the sphere, and E^* is the effective contact modulus given as,

$$\frac{1}{E^*} = \frac{1-\nu_1^2}{E_1} + \frac{1-\nu_2^2}{E_2} \tag{9}$$

where ν_i and E_i are the Poisson's Ratios and Elastic Moduli of the two contacting bodies, respectively. It is important to note here that, when the Hertzian elastic contact law is used alone, the COR, which is a measure of the severity of impact is always equal to unity. This is correct as long as the deformation is elastic and there are no viscous or plastic effects. However, it is well known, that in some cases there is energy loss due to plastic deformation or damage. For example, in case of metallic spheres, plasticity effects are present even for relatively low impact velocities (Goldsmith, 1960; Johnson, 1985; Lim & Stronge, 1998; Vu-Quoc & Zhang, 1999, Wu *et al*., 2003). Therefore, the Hertzian contact law has been used as part of more complicated contact laws that include damage effects due to plastic or permanent deformation. Such a nonlinear contact law and its linearized version are explained in detail in the following section.

Elastic-fully plastic contact law (flat spherical cap)

Experimental evidence suggests that during impact between metallic spheres, even at low impact velocities, the contact stresses are high enough to cause material yielding, and thus plastic deformation (Johnson, 1985).

In order to account for permanent deformation, an elastic-fully plastic contact law (Yigit & Christoforou, 1994) may be used to obtain the impact force. The contact law was obtained by combining the classical Hertzian contact theory (Goldsmith, 1960), and the elastic-fully plastic indentation theory given in Johnson (1985). The contact consists of three phases, with the first phase being elastic, where the contact is assumed to be Hertzian, the second phase being elastic-fully plastic, where the contact is assumed to exceed a threshold value and it includes both elastic and fully plastic deformation, and the third phase (unloading) being elastic. The contact law is given as follows:

Phase I: Elastic loading

$$F = K_h z^{3/2} \qquad 0 \le z \le z_p \tag{10}$$

Phase II: Elastic-fully plastic loading

$$F = K_p (z - z_p) + K_h z_p^{3/2} \qquad z_p \le z \le z_m \tag{11}$$

Phase III: Elastic unloading

$$F = F_m \left(\frac{z - z_f}{z_m - z_f} \right)^{3/2} \tag{12}$$

The transition from elastic to fully plastic loading occurs at indentation z_p, where fully plastic conditions are assumed. At the transition the contact force is given as,

$$F_p = \pi a_p^2 p_0 \tag{13}$$

where p_0 is the mean pressure, which remains constant within the contact region of radius a_p at fully plastic conditions. For metals, this begins to occur when $p_0 = 2.2 S_y$ where S_y is the yield strength of the target material (Goldsmith, 1960; Johnson, 1985; Yigit & Christoforou, 1994; Stronge, 2000). At fully plastic conditions the indentation and contact radius are related by,

$$z_p = \frac{a_p^2}{2R} \tag{14}$$

By combining Equations (13) and (14) the linear slope of the loading curve is given as,

$$K_p = 2\pi R p_0 \tag{15}$$

As it is well known initial yielding occurs well before and below the surface at $p_0 = 1.1 S_y$. There is a transition region that involves complicated force-deformation

relationships, which is between initial yield and fully plastic conditions (Stronge, 2000). In order to keep the contact law simple this region was ignored by matching the slope given by Equation (14) with the slope of the elastic loading curve given by Equation (10) at the transition indentation given as,

$$K_p = 2\pi R p_0 = 1.5 K_h \sqrt{z_p} \tag{16}$$

After some algebra the transition indentation is obtained as,

$$z_p = \frac{\pi^2 p_0^2 R}{E^{*2}} \tag{17}$$

After maximum indentation z_m and force F_m are reached, the unloading is elastic as prescribed by Equation (12). At the end of impact, the force is zero and the permanent deformation z_f is given as,

$$z_f = z_m - z_r \tag{18}$$

where z_r is the elastically recovered indentation given as (Goldsmith, 1960; Stronge, 2000),

$$z_r = z_p \left(\frac{2 z_m}{z_p} - 1 \right)^{1/2} \tag{19}$$

As mentioned above, for metallic spheres the transition to fully plastic conditions begins to occur at around two times the yield strength of the material where the contact pressure distribution remains constant. In the case of impact of sports balls, a similar behavior was observed (Cross, 1999; Stronge & Ashcroft, 2007), where the initially spherical ball flattens against the rigid surface. At the flattened stage of the ball, the contact force can be obtained similarly as in Equation (13), but with a more complicated expression of pressure and contact radius. By keeping the focus on balls with elastic cores and assuming elastic deformation up to the flattened configuration, the maximum contact pressure is assumed to be equal to the elastic stress at the contact point, which is estimated as,

$$p_0 = E \left(\frac{z_p}{R} \right) \tag{20}$$

By assuming similar behavior as in fully plastic conditions, that is constant mean pressure within the flat contact area, the transition indentation and contact stiffness at the onset of flattening can be obtained by substituting Equation (20) into Equations (16) and (17).

Linearized elastic-fully plastic contact law

In previous work it was shown that an elastoplastic contact law could be used effectively in the impact of compact bodies as well as flexible structures (Yigit & Christoforou, 1994; Christoforou & Yigit, 1998). Physically consistent results for the coefficient of restitution for the impact of spherical objects on thick composite laminates, and for the impact response of flexible structures with local contact damage were obtained. Furthermore, a linearized contact law was used to obtain simple and informative results for the non-dimensional response of structures (Christoforou & Yigit, 2009). The linear contact law, however, was elastic in nature and the effect of permanent deformation was neglected. Recently, a piecewise linear elastoplastic contact law, which was linearized at initial yielding was also proposed (Yigit *et al*., 2011). This linearization seems to have captured damage in brittle materials, such as fiber composites, but it under-predicted the contact force during yielding in metals. In response, a bi-linear contact law was suggested by linearizing the elastic-plastic loading and elastic unloading phases of the nonlinear elastic-fully plastic law given above (Christoforou *et al*., 2013). The two phases of the linearized contact law are given as follows:

Phase I: Loading

$$F = K_p z \tag{21}$$

Phase II: Unloading

$$F = F_m \left(\frac{z - z_f}{z_m - z_f} \right) \tag{22}$$

Normalized governing equations

It is usually convenient to present the results in a normalized form. Therefore, impact time, sphere displacement and impact force are normalized as follows:

$$\tau = \omega_0 t, \quad \overline{\alpha} = \frac{\alpha}{\upsilon_0 / \omega_0}, \quad \overline{F} = \frac{F}{m \upsilon_0 \omega_0} \tag{23}$$

where ω_0 is the linear contact frequency given as,

$$\omega_0 = \sqrt{\frac{K_p}{m}} \tag{24}$$

By introducing the linearized contact law into the equations of motion it is easy to show that the impact problem is governed by the following integral-differential equation given as,

$$\ddot{\alpha} + 2\zeta\omega_0(\lambda+1)\dot{\alpha} + \omega_0^2\alpha + 2\zeta\omega_0^3\lambda\int_0^t \alpha\, dt = 0 \tag{25}$$

where the two non-dimensional parameters, the relative stiffness, λ, and the damping factor, ζ, are given respectively as,

$$\lambda = \frac{K_r}{K_p}, \quad \zeta = \frac{\sqrt{mK_p}}{2c} \tag{26}$$

Furthermore, by using the normalized procedure, the integral-differential equation can be given in normalized form as,

$$\ddot{\bar{\alpha}} + 2\zeta(\lambda+1)\dot{\bar{\alpha}} + \bar{\alpha} + 2\zeta\lambda\int_0^\tau \bar{\alpha}\, d\tau = 0 \tag{27}$$

The initial conditions are now described as: $\bar{\alpha}(0) = 0$, and $\dot{\bar{\alpha}}(0) = 1$.

It should be noted here that although normalization is done using the linearized stiffness, it could be applied to the nonlinear equations as well with no difficulty. What is important is the insight provided by the normalized equations. For example, in the case of metallic spheres the relative stiffness could be unity or higher. Because of the high shear modulus the damping coefficient will be large resulting in a relatively small damping factor. This kind of impact will mainly be governed by the contact stiffness and the energy dissipation will be due to plastic deformation. On the other hand, in the case of sport balls the relative stiffness and the damping factor may vary significantly depending on the ball. For example, a superball will have relative stiffness close to unity, and a small damping coefficient resulting in a relatively large damping factor. This kind of impact will be governed by all the parameters, and the energy dissipation will mainly be due to damping. Furthermore, it is worth noting that when $\lambda \to 0$ the above equation reduces to the equation that governs the impact response of an infinite structure or a visco-elastoplastic sphere, which is given by the modified Maxwell model (Yigit *et al*., 2011; Ismail & Stronge, 2012), where the response is solely governed by the damping factor ζ. The governing equation is given as,

$$\ddot{\bar{\alpha}} + 2\zeta\dot{\bar{\alpha}} + \bar{\alpha} = 0 \tag{28}$$

As $\zeta \to 0$ the equation reduces further to that of an impact between compact bodies where the only energy dissipation is due to local plastic deformation. On the other hand for a specified λ, as $\zeta \to \infty$ Equation (27) reduces to the equation of a quasi-static type of impact where the response is solely governed by the relative stiffness, λ. In this case the governing equation is given as,

$$\ddot{\bar{\alpha}} + \left(\frac{\lambda}{\lambda+1}\right)\bar{\alpha} = 0 \tag{29}$$

The following simulations utilize examples from impact of some sport balls to demonstrate the applicability of the proposed model across a wide spectrum.

SIMULATION RESULTS AND DISCUSSION

In the following, the simulation results of the impact of various sports balls with a rigid flat surface are presented. The linearized equations of motion were solved numerically with the appropriate ball properties and initial conditions. The type of balls used, their properties and experimental measurements (Cross, 1999) are shown in Table 1.

Table 1. Experimental measurements of impact of sports balls.

Ball	**Mass**	**Radius**	**Impact velocity**	**COR**	**Max force**	**Contact time**
	m (g)	R (mm)	v_0 (m/s)	e	F_m (N)	t (ms)
Superball	37.4	21.55	3.12	0.75	121.8	3.0
Golfball	45.6	20.75	1.47	0.84	226.0	0.9
Baseball	143.6	35.25	1.25	0.49	289.0	2.2

Figure 2 shows the variation of the COR as a function of the two non-dimensional parameters ζ and λ. It presents the variation as a function of ζ for three values of λ, namely, $\lambda = 0$, $\lambda = 0.4$ and $\lambda = 1$. The simulations were carried out at a small and constant impact velocity to avoid plastic deformation, as it had been done in the experiments. Therefore, in Figure 2, only energy dissipation due to viscous or wave propagation is accounted for. For $\lambda = 0$, the COR varies with ζ as predicted by the modified Maxwell model. In the case of a specified λ, the COR initially decreases as a function of ζ, it reaches a minimum value and then it increases. It will eventually reach its quasi-static elastic impact value, which is equal to unity and where the response is independent of ζ. This will occur at large values of ζ, which is not practical for the small mass sports balls under study here. This figure clearly illustrates the effect of flexibility on the COR. For a given damping factor the higher the flexibility, the lower the COR. The model predictions agree well with the experimental data.

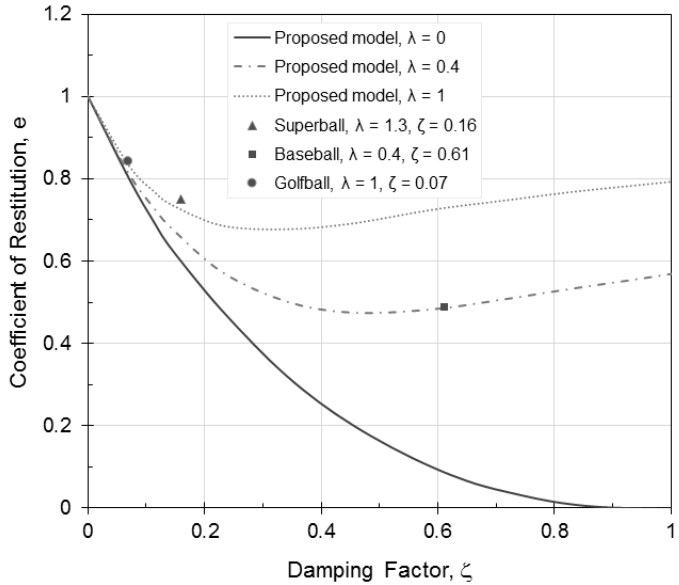

Fig. 2. Effect of damping and flexibility on the coefficient of restitution for various sports balls.

In order to demonstrate further the effect of the non-dimensional parameters on the impact response, the predicted normalized impact forces are placed as a function of λ and ζ on a characterization diagram that has been established in earlier work (Yigit & Christoforou, 2007), as shown in Figure 3. As it can be seen, the force response follows similar trends as the COR. Here, logarithmic scale is used in order to show large values of ζ and the complete dynamic spectrum.

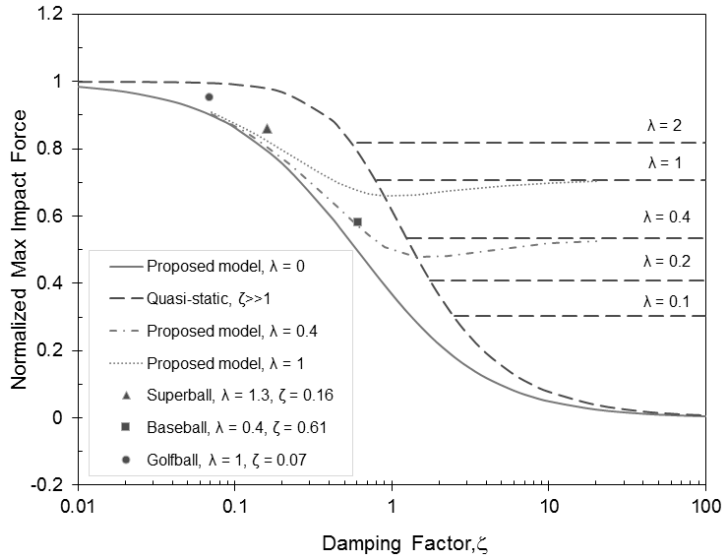

Fig. 3. Effect of damping and flexibility on the normalized maximum impact force for various sports balls.

In order to investigate the effect of flattening of the balls on the impact response, the impact velocity was increased substantially in the simulations. Figure 4 shows the effect of impact velocity on the COR. As it can be seen, the dependence of COR evolves as expected, that is at some critical velocity where plastic deformation or in this case flattening of the ball, the COR begins to decrease. As it was shown earlier, before the critical speed, the COR reduction is mainly due to wave propagation effects. However, at higher speeds the flattening area of the balls increases, with the ball remaining flattened after impact resulting in a lower COR. Ultimately, the ball will regain its original shape due to its recoil stiffness.

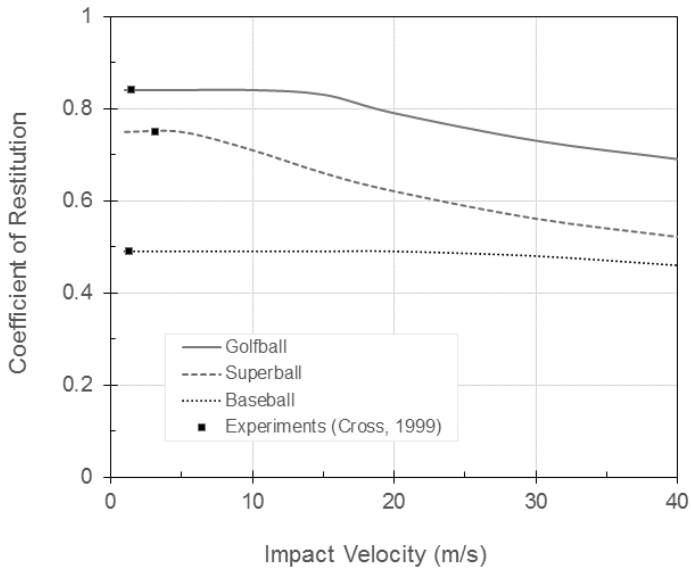

Fig. 4. Effect of impact velocity on the coefficient of restitution for various sports balls.

Also shown in Figures 2-4 are the experimental data of the COR and normalized maximum impact force for several sports balls (Cross, 1999). The non-dimensional parameters used for the balls in order to place the experimental data in the Figures, are shown in Table 2.

Table 2. Model parameters and predictions in impact of sports balls.

Ball	**Relative stiffness**	**Damping factor**	**COR**	**Max force**	**Contact time**
	λ	ζ	e	F_m (N)	t (ms)
Superball	1.3	0.16	0.75	117.3	2.8
Golfball	1.0	0.07	0.84	214.2	0.9
Baseball	0.4	0.61	0.49	276.8	1.6

As it will be explained below, for all cases, the non-dimensional parameters were calculated by Equation (26). Using the necessary and appropriate material and geometric properties, the damping coefficient c was calculated by using Equation (5), the contact parameters K_p and z_p were calculated by using Equations (15)-(20), and the recoil stiffness K_r was calculated to match the measured COR.

In the case of the superball the material density was calculated to be ρ = 892 kg/m^3 by using the mass and the radius of the ball given in Table 1. The elastic material properties used were E = 2.2 MPa for the modulus of elasticity and ν = 0.5 for the Poisson's ratio, which are common values used for the type of rubber material that the ball is made from (Callister & Rethwisch, 2011). By using Equation (5) the damping coefficient was calculated as c = 140 kg/s. Subsequently, by using Equations. (15), (17) and (20) the transition indentation was calculated as z_p = 4 mm, and the contact stiffness was calculated as K_p = 5.45 x 10^4 N/m. Following the procedure mentioned above, the recoil stiffness was obtained as K_r = 7.08 x 10^4 N/m to match the experimental COR. By substituting these parameter values into Equations (26) the non-dimensional parameters were calculated as ζ = 0.16 and λ = 1.3.

Figures 5 and 6 show the comparisons of the proposed model predictions and the experimental data for the impact response of a superball. As it can be seen the agreement is very good with nonlinear effects being evident, more so in the force-displacement response. The experimentally measured COR and the normalized maximum impact force were placed in Figures 2 and 3 using the calculated non-dimensional parameters. The proposed model prediction agrees with the experimental result exactly since the recoil stiffness value was selected to yield the same COR. As mentioned earlier, Figures 2 and 3 demonstrate the effects of flexibility of the impact response of the ball. When the effect of flexibility is significant, using the Maxwell model (λ = 0) as proposed by Ismail & Stronge (2012), may cause inconsistent interpretation of the results. By matching the impact force and COR they estimated the damping factor to be ζ = 0.01, which accounts for viscous effects, and the plastic loss factor to be γ = 0.78, which accounts for plasticity effects. These values would place the COR to the left of the curve for the Maxwell model shown in Figure 2. According to the model, it means that almost all lost energy is due to permanent indentation, which is not possible for a superball. Furthermore, using ζ = 0.01, the placement of the normalized maximum impact force ($\overline{F}_{mac} = 0.86$) in Figure 3 will not be in agreement with the predictions of the proposed model when λ = 0, because the normalized loading response and impact force are governed by the damping factor only (see Equation (28)). Moreover, by examining Figures 2 and 3 for the case at hand, the damping factor cannot be less than 0.1 and have consistent results for the COR and normalized impact force. Therefore, it is concluded that the energy loss reflected in the COR is due to wave propagation effects, with flexibility having major influence on the response, which is accounted for by the proposed model.

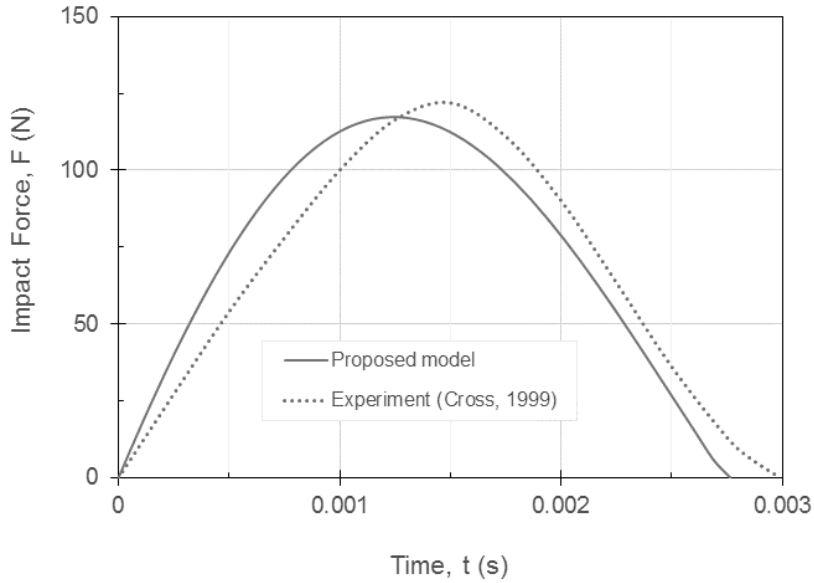

Fig. 5. Comparison of the proposed model prediction of force-time response with experimental measurement during impact of a superball with a rigid surface.

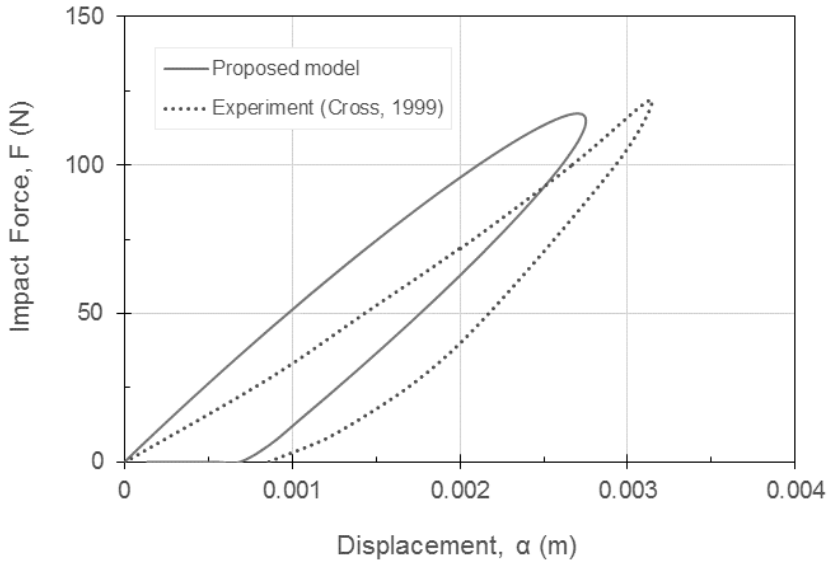

Fig. 6. Comparison of the proposed model prediction of force-displacement response with experimental measurement during impact of a superball with a rigid surface.

The second that is considered is the impact response of a golf ball. The estimation of the material parameters used for the simulations is more difficult, because the golf ball is a composite structure of three layers with different materials (Ismail & Stronge,

2008). The surface layer is made out of an elastomer resin having thickness $t = 2$ mm, density $\rho = 950$ kg/m^3, modulus of elasticity $E = 400$ MPa, and Poisson's ratio $\nu = 0.45$. The mantle, which is the second layer, is made out of Polybutadiene rubber having thickness $t = 5.4$ mm, density $\rho = 1155$ kg/m^3, modulus of elasticity $E = 50$ MPa, and Poisson's ratio $\nu = 0.43$. The core, which is the third layer, is made out of Titanium-Aluminum alloy (TI-6AL-4V) having thickness $t = 1.3$ mm, density $\rho = 4510$ kg/m^3, modulus of elasticity $E = 116$ GPa, and Poisson's ratio $\nu = 0.3$. Internally there is a spherical air gap, of approximately 12.05 mm radius, and with an assumed modulus of elasticity of 20.8 MPa. Following similar procedure as in the previous example, the transition indentation was calculated as $z_p = 3$ mm, the contact stiffness was calculated as $K_p = 5.6 \times 10^5$ N/m. The recoil stiffness was obtained as $K_r = 5.6 \times 10^5$ N/m to match the experimental COR. The composite modulus of elasticity that was used to estimate the contact stiffness was calculated by using the in-series spring analogy as,

$$\frac{1}{E} = \frac{1}{R}\sum_i \frac{t_i}{E_i} \tag{30}$$

By substituting the values of the three different layers plus the air-gap in Equation (30), the composite modulus was calculated to be 30 MPa. The Poisson's ratio was estimated as 0.4 by only using the three material layers in an equation similar to Equation (30). In order to estimate the damping factor, which depends on properties along the surface of the sphere, the parallel-spring analogy (rule of mixtures) was used as,

$$E = \frac{\sum_i t_i E_i}{\sum_i t_i} \tag{31}$$

A similar equation can be obtained for the density. By using only the first two surface layers in Equation (31), the modulus of elasticity along the surface was estimated to be 150 MPa and the density to be 1100 kg/m^3. These estimations resulted in damping coefficient $c = 1216$ kg/s. Finally, by substituting these parameter values into Equation (26) the non-dimensional parameters were calculated as $\zeta = 0.07$ and $\lambda = 1$. Figures 7 and 8 show the comparisons of the proposed model predictions and the experimental data for the impact response of a golf ball. As it can be seen the agreement is very good with nonlinear effects being less evident than in the case of the superball. As in the case of the super ball, the experimentally measured COR and the normalized maximum impact force were placed in Figures 2 and 3 using the calculated non-dimensional parameters. As before, the placement of the measured normalized maximum force in Figure 3 shows the effects of flexibility of the ball. In this case it is possible to use the Maxwell model ($\lambda = 0$) to obtain the response, if the model parameters are properly selected. It is concluded that in the case of the golfball the two models are in closer agreement with respect to the COR and the impact force.

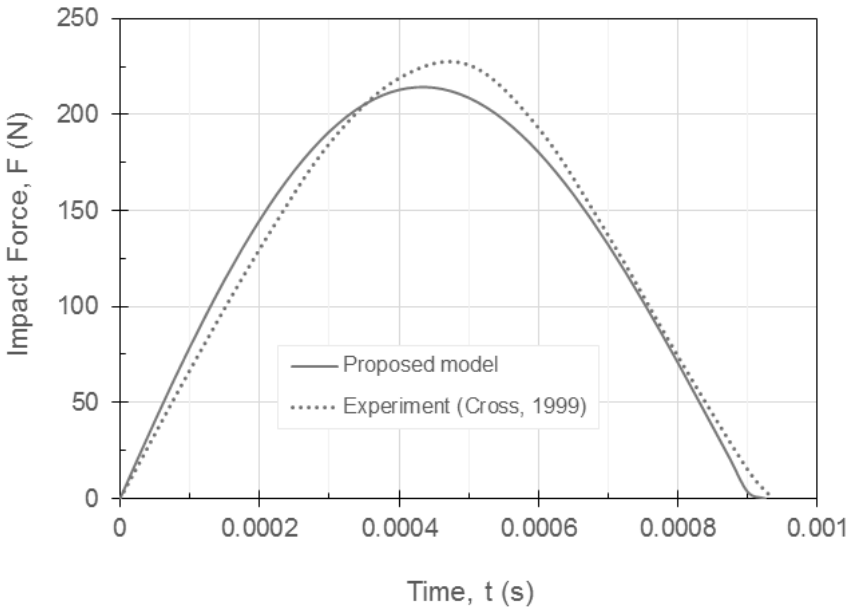

Fig. 7. Comparison of the proposed model prediction of force-time response with experimental measurement during impact of a golf ball with a rigid surface.

Finally, in the case of the baseball the material density was calculated to be $\rho = 783$ kg/m^3 by using the mass and the radius of the ball given in Table 1. The estimation of the properties is also difficult here as the surface of the baseball is made of thin leather and its core of cork. Therefore, an attempt was made to just match the COR and maximum impact force without paying particular attention to the details of the response. The elastic material properties used for the contact properties were $E =$ 40 MPa for the modulus of elasticity and $v = 0.4$ for the Poisson's ratio. Along the surface, in order to capture the wave propagation effect, $E = 2$ MPa was used, which is a common value for an elastomer (Callister & Rethwisch, 2011). By using Equation (5) the damping coefficient was calculated as $c = 320$ kg/s.

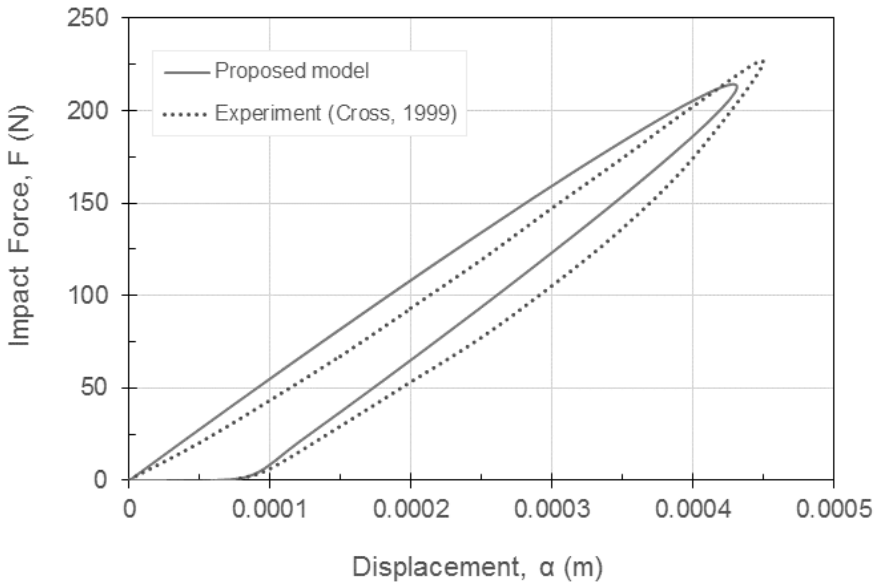

Fig. 8. Comparison of the proposed model prediction of force-displacement response with experimental measurement during impact of a golf ball with a rigid surface.

Subsequently, by using Equations (15), (17) and (20) the transition indentation was calculated as z_p = 5 mm, the contact stiffness was calculated as K_p = 10.5 x 10^5 N/m. Following the procedure mentioned above, the recoil stiffness was obtained as K_r = 4.2 x 10^5 N/m to match the experimental COR. By substituting these parameter values into Equation (26) the non-dimensional parameters were calculated as $\zeta = 0.61$ and $\lambda = 0.4$. The experimentally measured COR and the normalized maximum impact force were placed in Figures 2 and 3 using the calculated non-dimensional parameters. What it seems to be of interest here, is the placement of the measured COR in Figure 2. As it can be seen the flexibility of the ball has a major influence on the response. Therefore the simpler Maxwell model should not be used in the case of the baseball.

In closing, it is obvious from the results that the Maxwell model is adequate for small values of ζ, where flexibility does not play a major role. This will certainly be valid for metallic spheres, billiards and bowling balls. In the case of flexible sports balls, however, this model may not perform well in some cases. The proposed model can be a good alternative because in addition to wave propagation and local plastic deformation effects it includes the structural flexibility of the ball, which introduces a second non-dimensional parameter, the relative stiffness, λ.

CONCLUSIONS

An impact model that incorporates energy losses due to local plastic deformation, viscoelastic material behavior and wave propagation has been developed and used

to study the impact response of deformable spheres. The model also takes into consideration the structural deformation of the spherical object. Linearization of the governing differential equations and subsequent normalization has shown that the impact response of deformable spheres on a rigid surface is governed by two non-dimensional parameters, namely the relative stiffness λ, which accounts for structural recoil effects, plastic deformation and/or flattening of the sphere, and the damping factor, ζ, which accounts for viscous and/or wave propagation effects. It has been shown that the impact response and the COR are dependent on both parameters. At low speeds and damping factors the normalized impact force and COR mainly depend on damping; whereas, at large damping factors the flexibility of the sphere plays an important role as well. For a given damping factor, the normalized maximum impact force and COR decrease with higher flexibility. At higher speeds the COR decreases further due to surface flattening of the sphere. The model predictions have been compared to experimental data for a superball, a golf ball and a baseball with very good results. Based on the performance and safety needs of a particular sports ball, the non-dimensional parameters and their relationship to COR and maximum impact force, can be used in parametric studies to optimize performance and safety. It is expected that time and cost can be reduced in experimental and analytical/computational studies because the number of parameters of the problem has been reduced to two non-dimensional parameters.

REFERENCES

Alsakarneh, A., Quinn, B., Kelly, G. & Barrett, J. 2012. Modelling and simulation of the coefficient of restitution of the sliotar in hurling. Sports Biomechanics, **11**(3):342-357.

Callister, W.D. & Rethwisch, D.G. 2011. Materials Science and Engineering, eighth edition. John Wiley & Sons, Asia.

Christoforou, A.P. & Yigit, A.S. 1998. Effect of flexibility on low velocity impact response. Journal of Sound and Vibration, **217**:563-578.

Christoforou, A.P. & Yigit, A.S. 2009. Scaling of low-velocity impact response in composite structures. Composite Structures, **91**:358-365.

Christoforou, A.P., Yigit, A.S. & Majeed, M.A. 2013. Low-velocity impact response of structures with local plastic deformation: characterization and scaling. Journal of Computational Nonlinear Dynamics, **8**:011012-1, 011012-10.

Cross, R. 1999. The bounce of a ball. American Journal of Physics, **67**(3):222-227.

Goodwill, S.R., Kirk, R. & Haake, S.J. 2005. Experimental and finite element analysis of a tennis ball impact on a rigid surface. Sports Engineering, **8**:145-158.

Doyle, F.J. 1989. Wave Propagation in Structures: An FFT-based Spectral Analysis Methodology. Springer-Verlag, New York.

Goldsmith, W. 1960. Impact. Edward Arnold, London.

Hanly, K., Collings, F., Cronin, K., Byrne, E., Moran, K. & Brabazon, D. 2012. Simulation of the impact response of a sliotar core with linear and nonlinear contact models. International Journal of

Impact Engineering, **50**:113-122.

Hunt, K.H. & Crossley, F.R.E. 1975. Coefficient of restitution interpreted as damping in vibroimpact. Journal of Applied Mechanics, **42**(2):440-445.

Ismail, K.A. & Stronge, W.J. 2008. Calculated golf ball performance based on measured visco-hyperelastic material properties (P5). In: Estivalet M. & Brisson P. (Ed.). The Engineering of Sport 7-Vol 1. Pp. 11-18. Springer-Verlag, France.

Ismail, K.A. & Stronge, W.J. 2012. Viscoplastic analysis for direct impact of sports balls. International Journal of Nonlinear Mechanics, **47**:16-21.

Johnson, K.L. 1985. Contact Mechanics. Cambridge University Press, Cambridge.

Lim, C.T. & Stronge, W.G. 1998. Normal elastic-plastic impact in plane strain. Mathematical Computational Modelling, **28** (4-8):323-340.

Nevins, D. & Smith, L. 2013. Influence of ball properties on simulated ball-to-head impacts. Procedia Engineering, **60**:4-9.

Ranga, D. & Strangwood, M. 2010. Finite element modelling of the quasi-static and dynamic behavior of a solid sports ball based on component material properties. Procedia Engineering, **2**:3287-3292.

Smith, L. & Burbank, S. 2013. Simulating sport ball impact through material characterization. Procedia Engineering, **60**:73-78.

Stronge, W.J. 2000. Impact Mechanics. Cambridge University Press, Cambridge.

Stronge, W.J. & Ashcroft, A.D.C. 2007. Oblique impact of inflated balls at large deflections. International Journal of Impact Engineering, **34**:1003-1019.

Vu-Quoc, L. & Zhang, X. 1999. An elastoplastic contact force-displacement model in the normal direction: displacement-driven version. Proceedings: Mathematical, Physical and Engineering Sciences, **455**(1991):4013-4044.

Weir, G. & Tallon, S. 2005. The coefficient of restitution for normal incident, low velocity particle impacts. Chemical Engineering Science, **60**:3637-3647.

Wu, C.Y., Li, L.Y. & Thornton, C. 2003. Rebound behavior of spheres for plastic impacts. International Journal of Impact Engineering, **28**:929-946**.**

Yigit, A.S. & Christoforou, A.P. 1994. On the impact of a spherical indenter and an elastic-plastic transversely isotropic half-space. Composites Engineering, **4**(11):1143-1152.

Yigit, A.S. & Christoforou, A.P. 2007. Limits of asymptotic solutions in low-velocity impact of composite plates. Composite Structures, **81**(4):568-574.

Yigit, A.S., Christoforou, A.P. & Majeed, M.A. 2011. A nonlinear visco-elastoplastic impact model and the coefficient of restitution. Nonlinear Dynamics, **66**:509-521.

Zener, C. & Feshbach, H. 1939. A method of calculating energy loses during impact. Journal of Applied Mechanics, **61**:A67-A70.

Submitted: 01/10/2015
Revised: 06/12/2015
Accepted: 08/12/2015